Errata: "Introduction to Accelerator Dynamics"

Contents

0.1 Equation 1.7 (p 6)

$$X \;=\; \tilde{Y} / \left(\max_i \sum_j |Y_{ij}| \cdot \max_j \sum_i |Y_{ij}| \right)$$

until converged {

$$X \;=\; X + X(I - XY) \tag{0.1}$$

}

0.2 Exercise 1.6 (p 12)

The electron-proton collider HERA operated with two rings: one storing 30 GeV electrons, and the other storing 800 GeV protons. What was the centre-of-mass collision energy?

0.3 Text (p 19)

The integrated geometric strength of a thin quadrupole – the inverse of the focal length f – is proportional to L

0.4 Exercise 2.3 (p 22)

RHIC collides fully stripped gold ions with $(Z, A) = (79, 196.97)$ at a top energy of 100 GeV/nucleon in each beam, in rings of circumference 3834 m. The atomic mass unit is $m_0 = 0.93149$ GeV/c^2.

a) The injection energy is 10.5 GeV/nucleon. What is the required swing in revolution frequency during RHIC acceleration?

b) There are 192 main arc dipoles per ring, with a magnetic length $L = 9.42$ m. In the approximation that only they provide all 2π radians of bending, what is the dipole field at top energy?

0.5 Exercise 2.7 (p 22)

How is the matrix representing a linear magnet transformed when it is expressed in a coordinate frame (X, X') where $X = -x$, and $X' = -x'$?

0.6 Exercise 2.8 (p 22)

Figure 2.10 illustrates an early reel-to-reel tape drive, reading and writing data through an input/output channel to a nearby computer. The fluctuating data transfer rate determines the speed at which tape is fed through the magnetic pickup. The amount of loose tape sucked into nearby partial-vacuum buffers is sensed, turning on or off the motor or brake on the nearby reel, or allowing the reel to free-wheel. Assume that the sensors are perfect, and that the reel motor acceleration and brake deceleration rates are simple constants.

a) Is the system prone to uncontrolled oscillations that could break the tape? Under what conditions?

b) Clearly, this dynamical system is not readily amenable to representation by differential equations. Although numerical simulation is relatively straightforward, might it introduce artefacts that are not present in the real world?

c) Illustrate your answers with results generated by a numerical simulation.

0.7 Equation 3.6 (p 26)

$$\vec{x}_n \;=\; M^n\,\vec{x}_0 \;=\; A\lambda_1^n\vec{v}_1 \;+\; B\lambda_2^n\vec{v}_2 \tag{0.2}$$

0.8 Equation 3.31 (p 29)

$$M_{21} \;=\; \begin{pmatrix} \sqrt{\frac{\beta_2}{\beta_1}}\,(c_{21}+\alpha_1 s_{21}) & \sqrt{\beta_2\beta_1}\,s_{21} \\[2mm] \frac{-(1+\alpha_1\alpha_2)\,s_{21}+(\alpha_1-\alpha_2)\,c_{21}}{\sqrt{\beta_2\beta_1}} & \sqrt{\frac{\beta_1}{\beta_2}}\,(c_{21}-\alpha_2 s_{21}) \end{pmatrix} \tag{0.3}$$

0.9 Equation 3.35 (p 30)

The phase advance from s_1 to s_2 is found by inverting the equation

$$\tan(\phi_2-\phi_1) \;=\; \frac{m_{12}}{m_{11}\beta_1 - m_{12}\alpha_1} \tag{0.4}$$

giving an unambiguous result if the phase advance is not too large. See Equation A.32 for the particular case of propagation through a drift.

0.10 Exercise 3.5 (p 35)

Consider the net effect of axially symmetric convex and concave lenses on a light beam. If two lenses with focal lengths f and $-f$ are placed distance L apart, demonstrate that there is net focussing if $|f| > L$, no matter which way round the lenses are placed.

0.11 Exercise 3.7 (p 35)

Consider the FODO cell matrix

$$M \;=\; \begin{pmatrix} 1-2(qL)^2 & 2L(1+(qL)) \\ -2q(qL)(1-qL) & 1-2(qL)^2 \end{pmatrix} \tag{0.5}$$

a) Demonstrate directly that M is unitary.

b) What are the eigenvalues and eigenvectors of M? Why doesn't it matter that they are complex?

0.12 Equation 4.2 (p 37)

$$\delta \;=\; \frac{p-p_0}{p_0} \;=\; \frac{\Delta p}{p_0} \tag{0.6}$$

0.13 Equation 4.29 (p 44)

$$f_{RF} \;=\; \frac{\beta c}{\lambda_{RF}} \;=\; h f_{rev} \;=\; h\frac{\beta c}{C} \tag{0.7}$$

0.14 Equation 4.31 (p 44)

$$\delta_{n+1} \;=\; \delta_n \;+\; \left(\frac{qV_{RF}}{\beta^2 E_0}\right)\sin\left(2\pi\frac{z_{n+1}}{\lambda_{RF}}\right) \tag{0.8}$$

0.15   Equation 4.35 (p 45)

$$Q_s = \sqrt{\frac{|\eta_s|}{2\pi} \cdot \frac{C}{\lambda_{RF}} \cdot \frac{qV_{RF}}{\beta^2 E_0}} \tag{0.9}$$

0.16   Equation 5.13 (p 53)

$$\begin{pmatrix} \langle x^2 \rangle \\ \langle xx' \rangle \\ \langle x'^2 \rangle \end{pmatrix} = \epsilon_{x,u} \begin{pmatrix} \beta_x \\ -\alpha_x \\ \gamma_x \end{pmatrix} \tag{0.10}$$

0.17   Equation 5.17 (p 54)

$$\sigma^2_{x,TOT} = \beta_x \epsilon_{x,u} + \eta^2 \left(\frac{\sigma_p}{p_0} \right)^2 \tag{0.11}$$

0.18   Text Section number (p 55)

In summary, there is no structure in angle ϕ in the final distribution

$$\rho_{final}(J, \phi) = \rho_{final}(J) \approx N \, \delta(J - J_{inj}) \tag{0.12}$$

but the average action is increased from 1.25 nm to 21.25 nm. (See section 5.4 for a more exact discussion of injection errors.)

0.19   Potential subsection move (p 57)

Injection displacement and momentum errors Move this subsubsection to the end of subsection 5.3.

0.20   Equation 5.29 (p 57)

Thus, the total action of a particle that initially had action-angle co-ordinates (J, ϕ) at a location where $\alpha = 0$ becomes

$$J_T = J + \Delta x \sqrt{\frac{2J}{\beta}} \sin(\phi) + \frac{\Delta x^2}{2\beta} \tag{0.13}$$

0.21   Exercise 5.9 (p 62)

Multiple Coulomb scattering occurs as a beam passes through a thin beam instrumentation flag, adding an RMS angular divergence of

$$\bar{\theta} = \sqrt{\langle \theta^2 \rangle} \approx Z \left(\frac{20 \, [\text{MeV/c}]}{p\beta} \right) \sqrt{\frac{x}{L_{\text{rad}}}} \left(1 + \frac{1}{9} \log_{10} \frac{x}{L_{\text{rad}}} \right) \tag{0.14}$$

where Z is the beam particle charge, x is the flag thickness (traditionally measured in [g cm^{-2}]), and L_{rad} is the radiation length of the flag material. This increase in angular divergence enlarges the emittance.

A gold beam with a total energy of 10 GeV/nucleon passes through a 1 mm thick Al$_2$O$_3$ flag, at a location in a transfer line where $\beta = 6$ m and $\alpha = 0$. Assume that $L_{\text{rad}} = 24$ g cm^{-2} and $\rho_{\text{Al}_2\text{O}_3} = 3.7$ g cm^{-3}.

4

a) Evaluate $\bar{\theta}$.

b) If the normalised RMS emittance is $\epsilon_n = 2$ μm just upstream of the flag, what is the downstream emittance?

0.22 Equation 6.14 (p 68)

$$B_y + iB_x = G_0(I)(x + iy)\left(1 + 10^{-4}\sum_{n=2}^{\infty}(b_n + ia_n)\left(\frac{x+iy}{R_0}\right)^{n-1}\right) \qquad (0.15)$$

0.23 Exercise 6.4 (p 70)
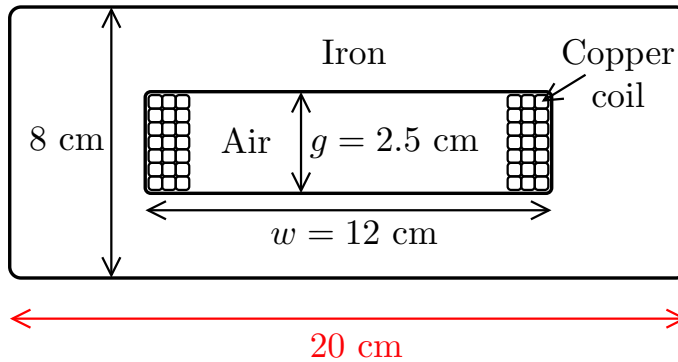
Use the Biot-Savart law to show that a thin cylindrical current shell distribution

$$J(r,\theta) = j_0\,\delta(r - a_0)\,\cos(n\theta) \qquad (0.16)$$

leads to a pure multipole inside a radius of a_0. (This is a challenging exercise.)

0.24 Exercise 6.6 (p 70)

Consider the window-frame dipole magnet shown in the figure, with gap width $w = 12$ cm, gap height $g = 2.5$ cm, and length $l = 1$ m.

a) Show that the magnetic field in the gap is

$$B = \mu_0\frac{NI}{g} \qquad (0.17)$$

where N is the number of turns and I is the current in each turn, if the iron has infinite relative permeability $\mu_r \equiv (\mu/\mu_0) = \infty$.

b) Show that the inductance of the magnet is

$$L = \mu_0 N^2\frac{lw}{g} \qquad (0.18)$$

c) If the resistivity of copper is ρ, and the cross sectional area of the copper in each of the two coils is A, what is the total power dissipation in the magnet?

d) How many ampere-turns (NI) are necessary to achieve a field of 0.6 T in the gap, if the relative permeability of the iron is $\mu_r = 5000$. What, approximately, is the maximum field in the iron? Where?

e) Air-cooled copper coils carry a maximum current density of about 1.5 A/mm^2, while water-cooled copper coils can carry almost 10 times as much. However, water-cooling adds the potential for water leaks and is more expensive, so it is avoided if possible. Would you recommend water-cooled or air-cooled coils for this magnet? How much horizontal space is available between the coils for a beampipe?

f) If the magnet power supply has a maximum current of 1000 A, how many turns should be used in the coil?

g) Calculate the inductance of the magnet. How much energy is stored in the gap? How much power is dissipated in the coils?

h) Assuming constant field in the iron, estimate the additional energy stored in the iron yoke.

0.25   Equation 7.2 (p 73)

$$
\begin{aligned}
\vec{E} &= \vec{E}(r,\theta)\, e^{i(kz-\omega t)} \\
\vec{B} &= \vec{B}(r,\theta)\, e^{i(kz-\omega t)}
\end{aligned}
\tag{0.19}
$$

0.26   Figure 7.2 (p 75)

0.27   Text function/parameter (p 85)

Suppose for simplicity that the Twiss parameter $\alpha_0 = 0$, so that

$$
I - M = \begin{pmatrix} 1-C & -\beta S \\ S/\beta & 1-C \end{pmatrix}
\tag{0.20}
$$

0.28   Equation 9.17 (p 97)

$$
\begin{pmatrix} \chi_x \\ \chi_y \end{pmatrix}_{GOAL} = \frac{1}{2\pi} \begin{pmatrix} \sum_F \eta\beta_x & \sum_D \eta\beta_x \\ \sum_F -\eta\beta_y & \sum_D -\eta\beta_y \end{pmatrix} \begin{pmatrix} S_F \\ S_D \end{pmatrix} + \begin{pmatrix} \chi_x \\ \chi_y \end{pmatrix}_{NAT}
\tag{0.21}
$$

0.29   Exercise 9.1 (p 104)

If the strength of a sextupole is g_p in physical phase space, so that [indexSextupole

$$
\begin{pmatrix} \Delta x'_p \\ \Delta y'_p \end{pmatrix} = -g_p \begin{pmatrix} x_p^2 - y_p^2 \\ -2x_p y_p \end{pmatrix}
\tag{0.22}
$$

show that kick in normalised phase space is

$$
\begin{pmatrix} \Delta x' \\ \Delta y' \end{pmatrix} = -\begin{pmatrix} (\beta_x^{3/2} g_p)\, x^2 - (\beta_x^{1/2}\beta_y g_p)\, y^2 \\ -2g(\beta_x^{1/2}\beta_y g_p)\, xy \end{pmatrix}
\tag{0.23}
$$

where β_x and β_y are the Twiss functions at the sextupole.

0.30   Equation 11.4 (p 117)

$$
P = \frac{1}{6\pi\epsilon_0} \cdot \frac{q^2 c}{\rho^2} \cdot \beta^4 \gamma^4
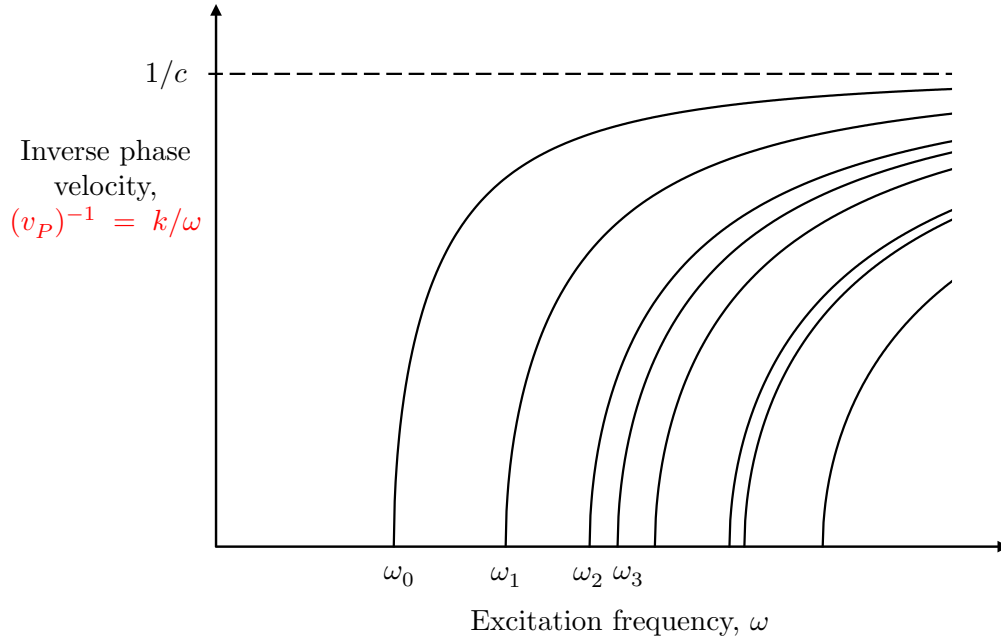\tag{0.24}
$$

Figure 1: The dependence of wave number k on excitation frequency ω for a family of TE or TM waveguide modes with cut-off frequencies ω_n.

0.31   Exercise 11.2 (p 129)

The Lorentz transformations of electromagnetic fields are

$$\vec{E'_\perp} = \gamma\,(\vec{E_\perp} + \vec{v} \times \vec{B_\perp}) \tag{0.25}$$

$$\vec{E'_\parallel} = \vec{E_\parallel} \tag{0.26}$$

$$\vec{B'_\perp} = \gamma\,(\vec{B_\perp} - \frac{1}{c^2}\vec{v} \times \vec{E_\perp}) \tag{0.27}$$

$$\vec{B'_\parallel} = \vec{B_\parallel} \tag{0.28}$$

where $\parallel$ labels the component of the field parallel to the boost velocity $\vec{v}$ and $\perp$ labels the perpendicular. Compute the electromagnetic fields of a singly charged particle traveling at relativistic velocity $\vec{v}$.

0.32   Exercise 11.8 (p 130)

(See also Exercisise 4.4 and 8.8.) RHIC accelerates fully-stripped gold ions in an RF system with a harmonic number of $h = 360$ and with a typical voltage of $V_{RF} = 300$ kV. Assume that transition $\gamma_T = 22.89$, and ignore synchrotron radiation.

a) If $\phi_s = 0°$ before acceleration begins, when $\gamma = 10.4$, what is the synchrotron frequency (in Hz)?

b) For a synchronous phase of $\phi_s = 5.5°$, how much energy does the synchronous particle gain per turn?

c) How long does it take to accelerate to $\gamma = 107.4$? Assume that the phase jump at transition has been performed correctly – ignore it.

d) Plot the synchrotron tune as a function of energy, up the acceleration ramp.

0.33 Text accurate/general (p 145)

To be accurate for general geometries the on-axis accelerating field E_z varies with z at a fixed time (except for a pill-box cavity), and so

$$T_1(\beta) = \frac{\int_{-L/2}^{L/2} E_z \cos(\omega t(z))\, dz}{\int_{-L/2}^{L/2} E_z\, dz} \tag{0.29}$$

0.34 Equation 13.17 (p 148)

$$L_e = -\frac{1}{mc^2}\frac{1}{\beta_r^3\gamma_r^3}\frac{2\pi(s_{n+1} - s_n)}{\lambda_{RF}} \tag{0.30}$$

0.35 Figure 13.8 (p 150)

The caption explanation for focusing/defocusing for Figure 13.8 is backwards. The field lines converge at the entry side (hence radially symmetric RF focusing at entry) and diverge at the exit side (hence radially symmetric RF defocusing at exit). The *focusing* effect dominates, because the exiting beam is more rigid.

0.36 Equation 13.30 (p 152)

$$\frac{1}{f_{net}} \approx +\frac{L}{f^2} \tag{0.31}$$

0.37 Figure 13.12 (p 156)

0.38 Text high/tight (p 157)

RFQs have significant advantages over the DC electrostatic systems that they superseded: continuous transverse electrostatic focusing is stronger than occasional magnetic focusing at slow speeds, efficient adiabatic bunching begins almost immediately out of the ion source, and the control parameters (L, a, m) are continuously optimised by machining the vanes. But RFQs also have their disadvantages: tight tolerances must be maintained in machining complex structures that are many meters long, thermo-mechanical stability is a challenge with higher power beams, and only one charge-to-mass ratio can be accelerated in a particular RFQ. Nonetheless, 10 MW-class proton linacs are only practical thanks to RFQ technology.
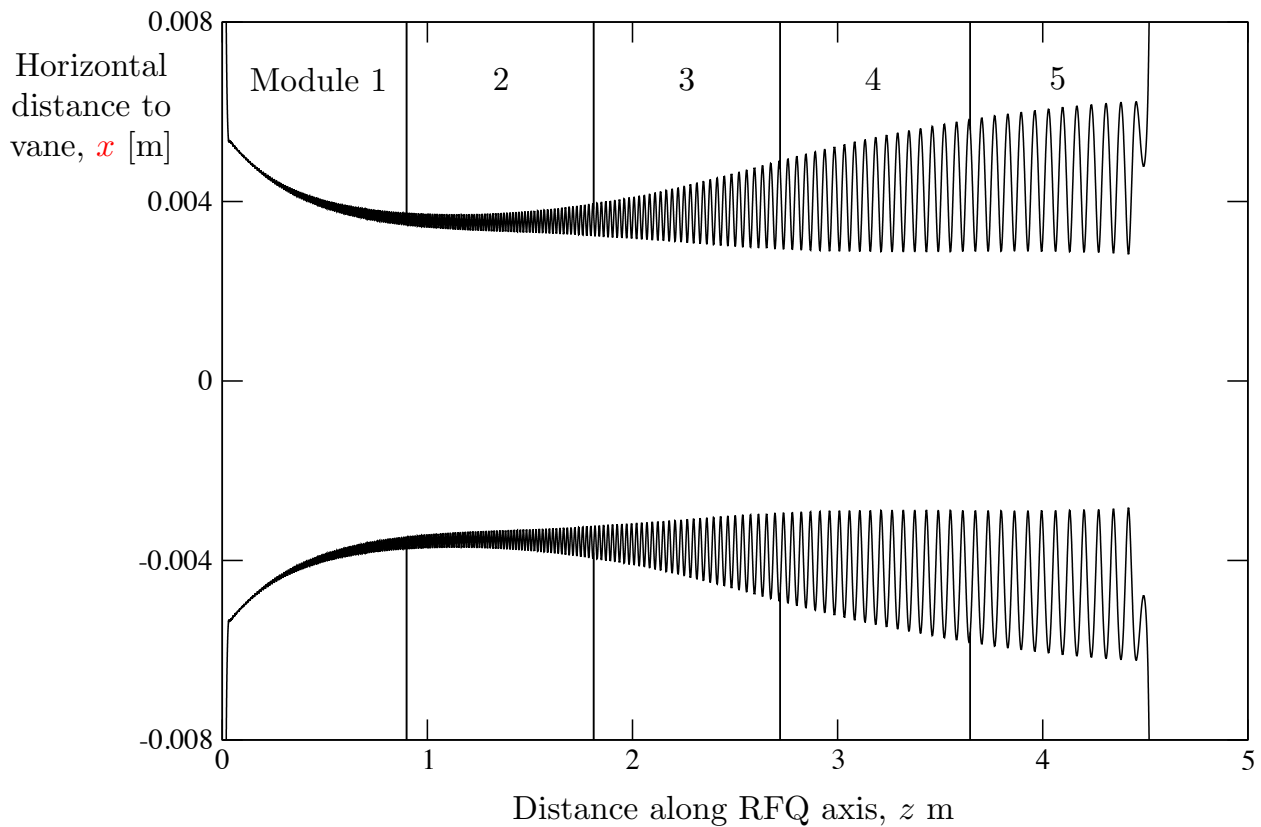
Figure 2: Longitudinal profile of the vanes in the ESS RFQ, showing the adiabatic evolution of the control parameters L, a, and m. The RFQ is assembled from 5 modules to form a single resonant cavity that is excited at 352 MHz. (Courtesy of A. Ponton.)

0.39 Equation 14.2 (p 160)

$$L_e = -\frac{1}{mc^2}\frac{1}{\beta_r^3\gamma_r^3}\frac{2\pi(s_{n+1}-s_n)}{\lambda_{RF}}$$ (0.32)

0.40 Exercise 14.1 (p 169)

Figure 3 sketches the layout of a simple four-dipole chicane in which the bend angle θ is small, and a is the distance between the first and second dipoles.
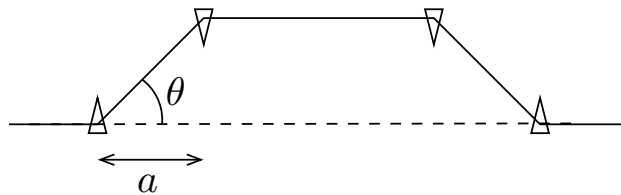

Figure 3: A simple four-dipole chicane, with no quadrupoles.

a) Following Equation 14.18, show that

$$M_{56} \equiv \frac{dz_2}{d\delta_1} = -2a\theta^2$$ (0.33)

9

b) Following the Taylor expansion of the path length in Equation **??**, show that

$$T_{566} = -\frac{3}{2}M_{56} \tag{0.34}$$

and

$$U_{5666} = 2M_{56} \tag{0.35}$$

c) At the front of the bunch is z negative or positive?